Supplemental Data for:

Nucleophilic Participation of the Reduced Flavin Coenzyme in the Mechanism of UDP-Galactopyranose Mutase

*He G. Sun, Mark W. Ruszczycky, Wei-chen Chang, Christopher J. Thibodeaux and Hung-wen Liu**

Division of Medicinal Chemistry, College of Pharmacy, Department of Chemistry and Biochemistry, and Institute of Cellular and Molecular Biology, University of Texas at Austin, Austin, Texas 78712

Contents

1 Overview

This Supplemental Data provides additional details regarding the controls, theory and statistical analysis described in the primary manuscript. Except for ^{13}C NMR peak deconvolution and integration, all data analysis was performed with programs written and implemented using the *GNU Octave* numerical analysis software, which is available as freeware at the website `www.gnu.org/software/octave` (1). Equation numbering follows that of the primary manuscript.

2 Linear free energy relationship

2.1 Estimation of steady state parameters

Steady state kinetic parameters were estimated according to the structural relation given by

$$v_i = \frac{V s_i}{K_M + s_i} \tag{2}$$

where v_i is the observed intial rate for each initial concentration, s_i, of UDP-Gal*f*. Nonlinear regression of (2) on the initial rate measurements was performed using the standard Gauss-Newton algorithm of iterative linearization assuming constant additive error (2, 3). Convergence was determined when the maximal change among the fitted parameters was less than 0.1%. The variance and covariance of each fitted parameter were obtained from the asymptotic variance-covariance matrix of the converged fit under the linear approximation (2, 3). The estimated standard deviation of each parameter, i.e., the standard error, is then the square root of the associated variance. It is well know that parameter confidence intervals are

underestimated by least-squares nonlinear regression methods (4, 5). Therefore, all confidence intervals and p-values should be considered nominal. Initial rates and corresponding fits using relation (2) are provided in Figure S1. The corresponding steady state parameters obtained from the fits are listed in Table S1.

Table S1: Steady state parameters obtained for the UGM catalyzed conversion of UDP-Gal$f$ to UDP-Gal$p$ following reconstitution with the different FAD analogues. Values of K_M and k_{cat}/K_M refer to the UDP-Gal$f$ substrate. The associated values of $\sigma = \sigma_m + \sigma_p$ are listed for both ionization of benzoic acid(σ_{BA}) (6) and phenylacetic acid (σ_{PA}) (7, 8). All values are reported $\pm$ one standard error.

FAD analogue	σ_{BA}	σ_{PA}	k_{cat} (s^{-1})	K_M (μM)	k_{cat}/K_M ($s^{-1}\mu M^{-1}$)	$\log_{10}(k_{cat})$	$\log_{10}(k_{cat}/K_M)$
FAD	-0.24	-0.22	14.9 ± 1.4	32 ± 9.6	0.46 ± 0.10	1.173 ± 0.041	-0.336 ± 0.094
8OMeFAD	-0.27	-0.12	8.0 ± 1.6	520 ± 180	0.0150 ± 0.0021	0.906 ± 0.089	-1.812 ± 0.59
7OMeFAD	0.12	0.13	4.59 ± 0.56	380 ± 85	0.0120 ± 0.0013	0.662 ± 0.053	-1.921 ± 0.047
8ClFAD	0.23	0.27	1.21 ± 0.23	130 ± 60	0.0089 ± 0.0025	0.083 ± 0.082	-2.05 ± 0.12
7ClFAD	0.37	0.37	1.23 ± 0.34	140 ± 100	0.0087 ± 0.0039	0.09 ± 0.12	-2.06 ± 0.19
7CF_3FAD	0.43	0.42	0.229 ± 0.022	25.8 ± 8.2	0.0088 ± 0.0022	-0.641 ± 0.042	-2.06 ± 0.11

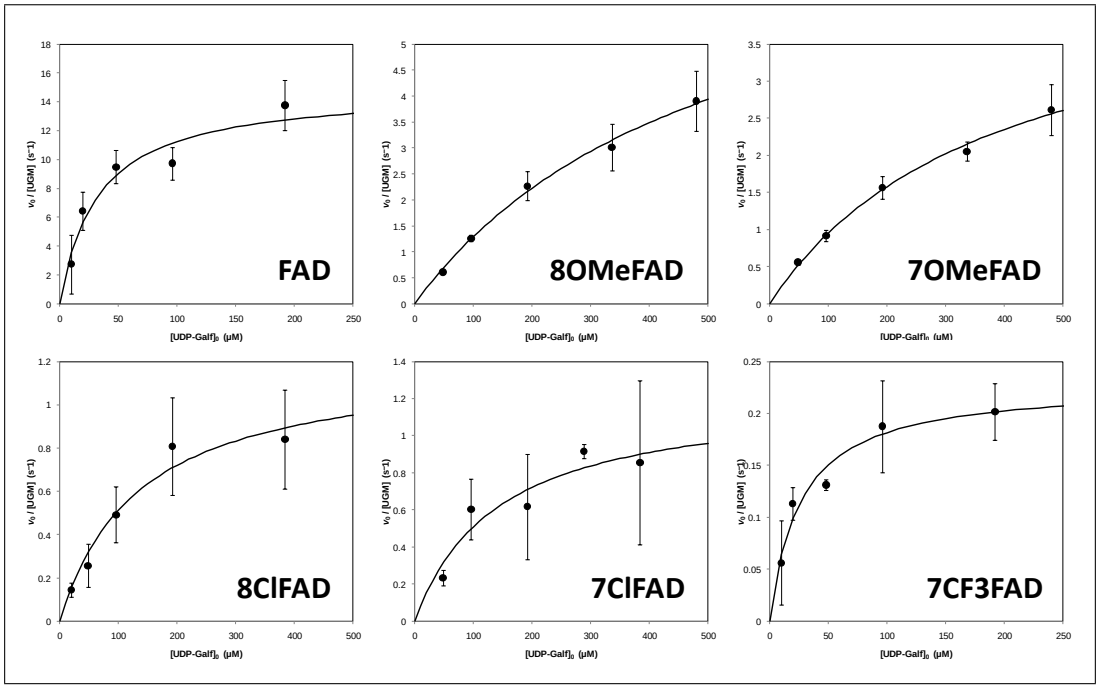

Figure S1: Plots of initial rate versus UDP-Gal$f$ concentration for the UGM catalyzed conversion of UDP-Gal$f$ to UDP-Gal$p$. Initial rates have been normalized for UGM concentration in the individual assays. Each initial rate is based on three replicate trials and error bars denote $\pm$ one standard deviation about the mean initial rate. Solid lines represent the fits to equation (2).

2.2 Estimation of ρ and hypothesis testing

2.2.1 Fitting the linear free energy relationship

The plot of $\log_{10}(k_{cat})$ versus σ, where $\sigma = \sigma_m + \sigma_p$, was initially performed using weighted linear regression, where the weights are proportional to the reciprocal variance of the $\log_{10}(k_{cat})$ estimates. These variances were determined via propagation from the variances of the k_{cat} estimates under a first order approximation.[1] The weighted fit is the more rigorous approach as it takes into account the relative uncertainty of each estimate of k_{cat} as well as the transformation of the variance

[1]Namely, using the conversion $\mathrm{var}(\log_{10}(k_{cat})) = (k_{cat}\ln(10))^{-2}\,\mathrm{var}(k_{cat})$.

incurred upon taking the logarithm. However, when plotting the data it was noted that the fitted line passed through only three of the six nominal 95% confidence intervals (not shown). This outcome has a low probability of 0.002, assuming the fitted line is a good approximation to the true relationship. This assessment is admittedly nonrigorous, because our choice of confidence interval is completely arbitrary and the confidence intervals are themselves underestimated due their ultimate origin from a nonlinear regression. Nevertheless, the result suggested that the error structure of the Hammett plot was not well defined according to the assumptions made on k_{cat}.

A possible explanation is that each analogue affects its associated k_{cat} in terms of both the electronic effects of interest as well as unrecognized and presumably random effects such as steric interactions within the active site that were otherwise not controlled for. These random effects would thus add another component to the error *in the LFER* in addition to that from the measurements themselves. Note that significant changes in rate limiting steps due to the LFER are expected to produce a systematic error, i.e., a curvature, for which there was no evidence (see Section 2.2.3 below). Due to this ambiguity, the LFER was also fit using unweighted least squares linear regression, which is the typical approach and effectively ignores the error in each value of k_{cat} and $\log_{10}(k_{cat})$, as well as the distribution-free method of Theil with confidence intervals determined according to Sen (9, 10).

Table S2: Estimates of ρ for the LFER between $\log_{10}(k_{cat})$ and $\sigma = \sigma_m + \sigma_p$ using different fitting algorithms. Values of ρ_{PA} versus ρ_{BA} were determined, respectively, using the σ_{PA}- versus σ_{BA}-sets of values for σ. The estimates of ρ are provided with the associated standard error and nominal 95% confidence interval. Note that distribution-free analysis provides only a confidence interval.

Fitting Algorithm	ρ_{PA}	95% conf. int. for ρ_{PA}	ρ_{BA}	95% conf. int. for ρ_{BA}
weighted least squares	-2.683 ± 0.086	$(-2.92, -2.44)$	-2.484 ± 0.080	$(-2.70, -2.26)$
unweighted least squares	-2.36 ± 0.44	$(-3.59, -1.13)$	-2.02 ± 0.44	$(-3.25, -0.79)$
distribution-free	-2.38	$(-4.49, -1.46)$	-2.21	$(-4.20, -0.63)$

The estimated susceptibility factors, ρ, for all three approaches with their standard errors and nominal 95% confidence intervals are listed in Table S2. When determining the LFER, two sets of σ values were considered, the first being the common "Hammett" set obtained via the ionization of benzoic acid in water, denoted σ_{BA} (6, 11). The second set is based on the ionization of phenylacetic acid in water, and is denoted here as σ_{PA} (or in other works as σ^0) (7, 8, 12). It has been proposed that *para*-substituted π-donor substituents can produce a transquinoidal resonance structure with benozoic acid leading to anomalous values of σ (12). For this reason the σ_{PA}-set was considered more reliable than the σ_{BA}-set, and indeed did provide more consistent LFER plots. The following analysis will, therefore, focus on the LFER obtained with the σ_{PA}-set. Nevertheless, the results with the σ_{BA}-set were similar as shown in Table S2 to the extent that the same conclusions were reached with both sets of σ values.

There are at least three key points. First, the values of ρ_{PA} (hereafter referred to simply as "ρ") are all very similar ranging from -2.68 to -2.36. Second, the nominal 95% confidence intervals do not include zero for any of the fitting algorithms. This implies that the negative correlation is indeed signficant at the nominal 5% significance level. Additionally, the p-value for the unweighted fit, i.e., the probabilty of observing $\rho < -2.36$ (or $\rho > 2.36$) assuming ρ in fact is equal to zero, is less than 0.006 according to a two-tailed t-distribution. Third, the standard error from the unweighted least squares fit is more than five-fold larger than that from the weighted least squares fit. This is consistent with the hypothesis of an additional component to the error discussed above. Based on these results we concluded that the most appropriate approach to the data was the unweighted least squares fit. The reasons for this are: 1. A likely additional, random component to the error beyond that of the measurement itself, which is accounted for better by the unweighted fit; and 2. A value of ρ very similar to that from the distribution-free fit. Nevertheless, the underlying assumptions discussed above should be kept in mind as would be the case with all LFER expriments — particularly in complicated systems such as those involving an enzyme active site.

2.2.2 Test for nonequivalence of ρ_m and ρ_p

It is well known that LFERs associated with *meta*- versus *para*-inductive effects are not necessarily equal, i.e., in general one expects $\rho_m \neq \rho_p$ (11). Furthermore, it has been suggested by Edmondson and Ghisla that this may be especially true for flavin analogues and in particular with regards to redox potentials (13). Therefore, to test the hypothesis that $\rho_m \neq \rho_p$ versus the null hypothesis that $\rho_m = \rho_p$ an analysis of variance (ANOVA) was performed. This ANOVA used unweighted

regressions consistent with the conclusions of Section 2.2.1 to compare the following two models,

$$y = y_0 + \rho(\sigma_m + \sigma_p) \tag{3a}$$

$$y = y_0 + \rho_m\sigma_m + \rho_p\sigma_p \tag{3b}$$

where y stands in for $\log_{10}(k_{cat})$ to simplify the notation, and y_0 is an intercept term, which simply permits the LFER to have a non-zero intercept. The fitted parameters for each of the two models are provided in Table S3.

Table S3: Parameters estimated based on the models in (3). All parameters are reported ± standard error. The total number of data points, N, is six in each case. The degrees of freedom, n, is the number of data points less the number of estimated parameters. The sum square residual, SSR, is also provided as well as the mean square residual, $MSR = SSR/n$. The estimated standard deviation about the regression is just $\sqrt{MSR}$. Fits were obtained using the σ_{PA}-set of σ values. Values are reported to four decimal places for computational purposes, i.e., to avoid rounding errors.

model	y_0	ρ	ρ_m	ρ_p	n	SSR	MSR
(3a)	0.7135 ± 0.1235	-2.3629 ± 0.4431	—	—	4	0.2713	0.0678
(3b)	0.7294 ± 0.1515	—	-2.4753 ± 0.6420	-2.1524 ± 0.8977	3	0.2642	0.0881

Our goal is to test the hypothesis that $\rho_m \neq \rho_p$ against the null hypothesis that $\rho_m = \rho_p$ using a one-tailed F-test (see Chapter 9 of Draper and Smith (5)). The best estimate of the variance about the regression[2] is given by the MSR of the larger model (3b), i.e., $MSR_{(3b)} = 0.0881$. The sum of squares due to the hypothesis $\rho_m \neq \rho_p$ is equal to $SSR_{(3a)} - SSR_{(3b)} = 0.0071$ having one degree of freedom. Therefore, the variance due to the hypothesis $\rho_m \neq \rho_p$ is $0.0071/1 = 0.0071$. If the hypothesis $\rho_m \neq \rho_p$ were true, then applying it should account for a significant amount of the observed variation beyond that due to simple error about the regression, which is best estimated from $MSR_{(3b)}$. The corresponding F-statistic is thus $F_{1,3} = 0.0071/0.0881$, which is less than unity and, therefore, insignificant ($F_{1,3}^{95\%} = 10.1$). In other words, the variance accounted for by the hypothesis $\rho_m \neq \rho_p$ is not significantly greater than the best estimate of the variance about the regression and, hence, does not improve the regression. Therefore, we cannot reject the null hypothesis ($\rho_m = \rho_p$) with the present data set.

2.2.3 Test for nonadditivity of σ_m and σ_p, i.e., curvature

It is also important to consider nonadditivity in the free energy relationship between $\log_{10}(k_{cat})$ and $\sigma = \sigma_m + \sigma_p$, i.e., curvature. To test for curvature we consider the following three models,

$$y = y_0 \tag{4a}$$

$$y = y_0 + \rho_1\sigma \tag{4b}$$

$$y = y_0 + \rho_1\sigma + \rho_2\sigma^2 \tag{4c}$$

Note that model (4a) is equivalent to an arithmetic average and model (4b) is the same as model (3a) discussed in the previous section. The structural relations (4) were fit to the data using unweighted least squares linear regression, and the estimated parameters and associated standard errors are listed in Table S4. To determine whether the fit provided by model (4c) is significant, an ANOVA was performed using the sequential sum square residuals technique to determine the significance of regression of each successive model (see Chapter 6 of Draper and Smith (5)).

The ANOVA for significance of regression is provided in Table S5. Line 3 describes the total variation after correcting for a non-zero mean obtained from model (4a). Line 2 describes the total variation after accounting for first and second order dependence on σ obtained from model (4c). The MSR of this largest model is used to provide the best estimate of the true variance about the regression. Line 1 describes the variance accounted for upon switching from model (4a) to model (4c). It therefore tests the hypothesis of model (4c) versus the null hypothesis of model (4a).[3] The corresponding $F_{2,3}$-statistic of 17.8 is significantly greater than unity ($p = 0.02$), again establishing a dependence of $\log_{10}(k_{cat})$ on σ. Lines 1a and 1b decompose the variance described by line 1 into that accounted for by the first (line 1a) and second (line 1b) order terms. The F-test of line 1a demonstrates the significance of the first order term ($p = 0.01$), and is redundant with the t-test described in Section 2.2.1.[4]

[2] This would stem entirely from error in the ability to measure k_{cat} if no other "random" components to the error were present, e.g., from steric effects.

[3] More correctly stated, the hypothesis of dependence versus no dependence on σ using model (4c) to represent "dependence".

[4] In fact, when model (4b) is used as the best estimate of the true variance about the regression, the one-tailed F-test described here and the two-tailed t-test of Section 2.2.1 are *exactly* equivalent as predicted by theory (5).

Table S4: Parameters estimated based on the models in (4). All parameters are reported ± standard error. The total number of data points, N, is six in each case. The degrees of freedom, n, is the number of data points less the number of estimated parameters. The sum square residual, SSR, is also provided as well as the mean square residual, $MSR = SSR/n$. The estimated standard deviation about the regression is just $\sqrt{MSR}$. All fits utilized the σ_{PA} set of σ values. Values are reported to four decimal places for computational purposes, i.e., to avoid rounding errors.

model	y_0	ρ_1	ρ_2	n	SSR	MSR
(4a)	0.3787 ± 0.2708	—	—	5	2.2002	0.4400
(4b)	0.7135 ± 0.1235	-2.3629 ± 0.4431	—	4	0.2713	0.0678
(4c)	0.8856 ± 0.1722	-1.6784 ± 0.6567	-3.4651 ± 2.6125	3	0.1710	0.0570

Line 1b describes the variation accounted for by the second order term, i.e., model (4c), that is not accounted for by model (4b). Line 1b thus tests the hypothesis of curvature versus the null hypothesis of linearity.[5] The corresponding $F_{1,3}$-statistic of 1.76 is too close to unity to suggest that the second order term is accounting for any variance beyond that from about the regression alone. Therefore, the second order regression is not signficant versus the first order ($p = 0.3$), and we cannot reject the null hypothesis of line 1b.

Table S5: Analysis of variance based on sequential sum square residuals to test for significance of regression upon adding higher order terms to the linear free energy relationship, i.e., models (4). See Table S4 for the results of the model fitting considered in the ANOVA. Values are reported to four decimal places for computational purposes, i.e., to avoid rounding errors.

Line	Source of Variation	n	SSR	MSR	F	p
1	Regression $\|y_0$	2	2.0292	1.0146	17.8	0.02
1a	Due to $\rho_1\|y_0$	1	1.9289	1.9289	33.8	0.01
1b	Due to $\rho_2\|\rho_1, y_0$	1	0.1003	0.1003	1.76	0.28
2	Residual	3	0.1710	0.0570	—	—
3	Total (corrected)	5	2.2002	0.4400	—	—

3 Positional isotope exchange

3.1 PIX time course experiments and determination of f

As discussed in the primary text, the C1 ^{13}C NMR signal of UDP-Gal*p* is split into a doublet by the adjacent β-phosphate and demonstrates an upfield shift of approximately 0.03 ppm when the anomeric oxygen is replaced with ^{18}O (14). Following peak deconvolution as described in the primary text, the observed value of f, i.e., the fraction of UDP-Gal*p* containing ^{18}O at the anomeric oxygen, was computed by dividing the sum of the two $^{13}\text{C1} - ^{18}\text{OP}_\beta$ peak integrations by the sum of the four peak integrations from both the $^{13}\text{C1} - ^{18}\text{OP}_\beta$ and $^{13}\text{C1} - ^{16}\text{OP}_\beta$ doublets. An example ^{13}C NMR spectrum is provided in Figure S2A along with the deconvolution. Also shown in Figure S2 are the ^{13}C NMR stack plots acquired during the PIX experiments with apo-UGM and 5-deaza-FAD/UGM.

Measurements of f from a single sample showed slight variation between days, for example due to shimming etc., and likely between instruments (see Section 3.3). The value of f_0, i.e., the total ^{18}O enrichment in doubly labeled UDP-Gal*p*, was determined from a single sample measured twice ($N = 2$) using the 600 MHz NMR on two separate consecutive days. The measurements of 0.729 (day one) and 0.816 (day two) yielded a mean value of 0.772 with a sample standard deviation (s) of 0.062 and standard error ($s/\sqrt{N}$) of 0.044. The former represents the variability between measurements, while the latter denotes the precision with which f_0 is estimated.

[5] More correctly stated, the hypothesis of nonlinear versus linear dependence on σ using model (4c) to represent "nonlinear dependence".

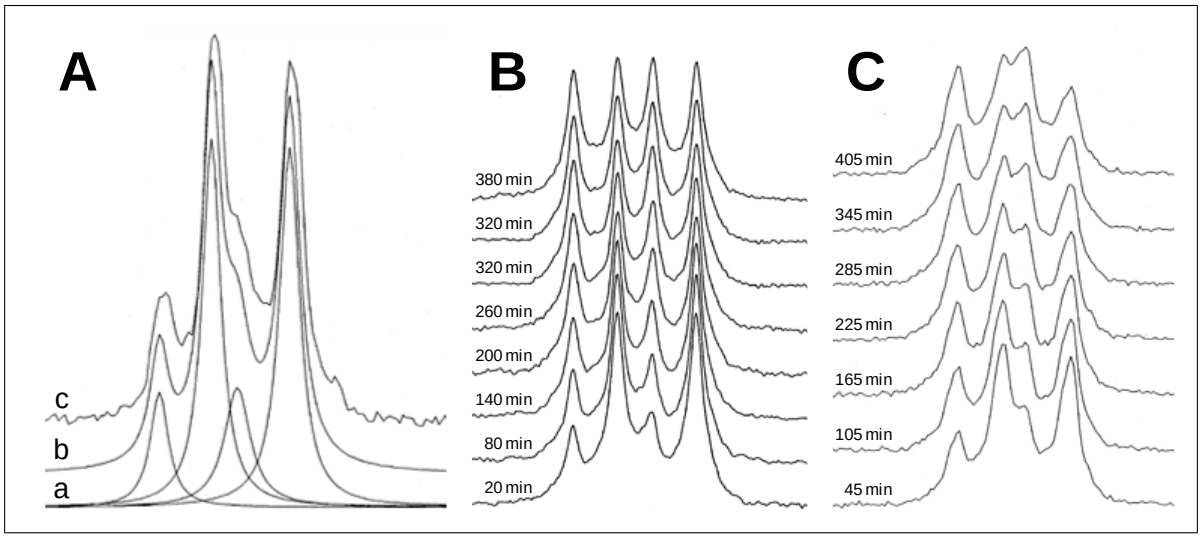

Figure S2: Collection of ^{13}C NMR spectra used to determine fractional enrichment of ^{18}O at the bridging position in UDP-[1-^{18}O,1-^{13}C]Gal*p*. A, 600 MHz ^{13}C NMR of doubly labeled substrate with the deconvoluted peaks (a), composite (b) and observed spectrum (c). B, 500 MHz ^{13}C NMR spectra obtained during PIX equilibration of the doubly labeled substrate in the presence of apo-UGM. C, 600 MHz ^{13}C NMR spectra obtained during PIX equilibration of the doubly labeled substrate in the presence of UGM reconstituted with 5-deaza-FAD. Note the improved peak separation in the 500 MHz spectra compared to the 600 MHz spectra.

3.2 Parameter estimation for PIX equilibration

Given the saturating total substrate concentration used in the PIX experiments, the apparent first order rate constant for positional isotope exchange, i.e., k_{PIX}, is equivalent to the maximal positional exchange rate (15), V_{ex}, divided by the total substrate concentration,

$$k_{PIX} = V_{ex}/s_0 \tag{5}$$

Therefore, k_{PIX}, is dependent on both total substrate and enzyme concentration, which was equivalent for the apo and 5-deaza-FAD experiments. In order to estimate k_{PIX}, observed values of f were fit using the exponential structural relation given by

$$f = f_{eq} + \Delta f \exp(-k_{PIX} t) \tag{1}$$

Fitting employed the standard Gauss-Newton algorithm of iterative linearization assuming constant additive error (3). Convergence was determined when the maximum change in the parameters between iterations was less than 0.001%. The parameter f_{eq} was fixed at the value 0.25745, equal to the initial ^{18}O enrichment multiplied by the statistical factor for partitioning of ^{18}O into the bridging position at PIX equilibrium. This parameter was fixed in order to better condition the model for estimating k_{PIX} from the observed data. The parameter Δf was allowed to float along with k_{PIX} to accomodate small variations in relative NMR peak integrations observed between days and instruments (see Sections 3.1 & 3.3). Standard errors of the estimated parameters, k_{PIX} and Δf, were obtained from the asymptotic variance-covariance matrix of the converged fit according to the linear approximation (3). As in the case of fitting the Michaelis-Menten equation (2), these nonlinear regression methods tend to underestimate the confidence intervals such that all p-values and confidence intervals should be considered nominal (4, 5).

An estimate of k_{PIX} for holo-UGM was obtained from the observation of approximately 31% labeling of ^{18}O at the bridging position after a 20 min incubation with 10 μM UGM reconstituted with FAD_{red}. Using the parameters $f_{eq} = 0.257$ and $\Delta f = 0.514$, in equation (1), one obtains $k_{PIX} \approx 0.112\ \text{min}^{-1}$. As the concentration of UGM in this control was two-thirds that in the reactions with apo enzyme or enzyme reconstituted with 5-deaza-FAD, the k_{PIX} estimate should be multiplied by a factor of 1.5. The final adjusted estimate is then $0.17\ \text{min}^{-1}$ at 15 μM enzyme, which is approximately 100-fold greater than the observed values of k_{PIX} determined for apo-UGM and UGM reconstitued with 5-deaza-FAD.

Despite attempts to completely remove FAD from the as-isolated UGM, the PIX results suggested that the apo-UGM still contained an experimentally observable level ($< 1\%$) of residual holo-enzyme. To control for this possibility, HPLC analysis of the reaction mixtures was performed to determine whether the UDP-Gal*f* product was being formed under the PIX experimental conditions in the presence of 5-deaza-FAD/UGM. The corresponding HPLC traces are shown in Figure S3.

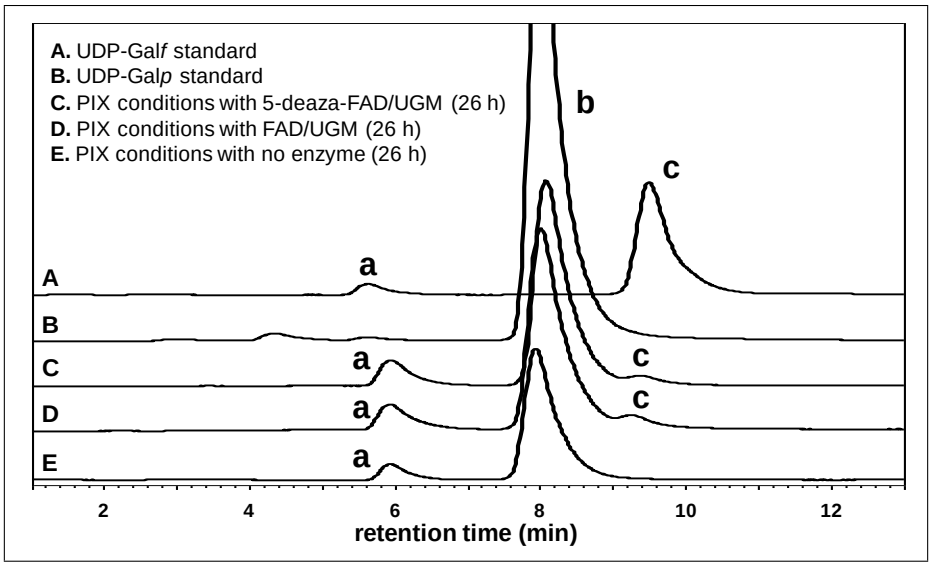

Figure S3: HPLC chromatograms to test for formation of UDP-Gal*f* during the PIX experiment with UGM reconstituted with 5-deaza-FAD. Peak a is uridine monophosphate (UMP), peak b is the UDP-Gal*p* substrate and peak c is the UDP-Gal*f* product. Incubations corresponding to traces C, D and E were conducted under PIX conditions for 26 h before HPLC analysis. As the HPLCs were run on different days, i.e., following the individual PIX experiments, there was some variability in retention time; therefore, the traces have been shifted along the abscissa to facilitate comparison. HPLC conditions are the same as those described in the primary text.

As can be seen from the traces, following a 26 h incubation a small peak with a retention time consistent with that of UDP-Gal*f* is observed with UGM when reconstituted with either FAD_{red} or 5-deaza-FAD (traces C and D, peak c), but not when enzyme is absent (trace E). Despite some overlap of the UDP-Gal*f* peak with the tail of the UDP-Gal*p* peak, peak integrations indicated ca. 5% conversion in the former two cases. This is consistent with the previously reported fractional conversion of ca. 7% at equilibrium (14).

3.3 Hypothesis testing

The values of k_{PIX} and Δf determined for apo-UGM versus UGM reconstituted with 5-deaza-FAD were compared according to a two-tailed *t*-test. The results are provided in Table S6. While the difference between the values of k_{PIX} is not significant, the difference between the values of Δf is significant. The latter result indicates that measurements of a single value of f can be expected to differ depending on the NMR instrument utilized as well as the day on which the measurement was made. The difference of 0.07 is consistent with the standard deviation described above in Section 3.1.

Table S6: Comparison of k_{PIX} and Δf for apo-UGM versus 5-deaza-UGM according to a two-tailed *t*-test. Each fit involved $N = 7$ time points and two parameters for $n = 5$ degrees of freedom each. The mean square residual about each regression (MSR_{fit}) was 1.49×10^{-4} and 1.30×10^{-4} for apo-UGM and 5-deaza-UGM, respectively, and these were pooled to obtain $MSR_{pooled} = 1.40 \times 10^{-4}$. The pooled variance of each parameter takes this improved estimate into account according to $s^2 = s^2_{fit} MSR_{pooled} / MSR_{fit}$.

Parameter	k_{PIX}		Δf	
Experiment	apo-UGM	5-deaza-UGM	apo-UGM	5-deaza-UGM
Estimate	1.54×10^{-3} min^{-1}	1.71×10^{-3} min^{-1}	0.435	0.505
Difference (Δ)	1.70×10^{-4} min^{-1}		0.0697	
Variance (s^2_{fit})	1.44×10^{-8} min^{-2}	1.21×10^{-8} min^{-2}	1.05×10^{-4}	1.26×10^{-4}
Pooled variance (s^2)	1.35×10^{-8} min^{-2}	1.30×10^{-8} min^{-2}	9.86×10^{-5}	1.36×10^{-4}
Variance of Δ	2.65×10^{-8} min^{-2}		2.35×10^{-4}	
t_Δ	1.04		4.55	
$t_{95\%}$ ($n = 10$)	2.23		2.23	
p ($n = 10$)	0.32		0.001	

References

1. Eaton, J. W. (2002), *GNU Octave Manual*, Network Theory Limited
2. Cleland, W. W. (1967), *Adv. Enzymol.* **29**, 1–32
3. Seber, G. A. F. and Wild, C. J. (2003), *Nonlinear Regression*, Wiley-Interscience, New Jersey
4. Johnson, M. L. (1994), *Method. Enzymol.* **240**, 1–22
5. Draper, N. R. and Smith, H. (1998), *Applied regression analysis*, Wiley-Interscience, New York, 3^{rd} edition
6. Hansch, C., Leo, A., and Taft, R. W. (1991), *Chem. Rev.* **91**, 165–195
7. Taft, R. W. J., Ehrenson, S., Lewis, I. C., and Glick, R. E. (1959), *J. Am. Chem. Soc.* **81**, 5352–5361
8. Ritchie, C. D. and Sager, W. F. (1964), in Cohen, S. G., Streitweiser, A., and Taft, R. W., eds., *Prog. Phys. Org. Chem.*, volume 2, pp. 323–400
9. Theil, H. (1950), *Proc. Kon. Nederl. Akad. Wetensch. A* **53**, 386–392, 521–525 & 1397–1412
10. Sen, P. K. (1968), *J. Amer. Statist. Assoc.* **63**, 1379–1389
11. Lowry, T. H. and Richardson, K. S. (1987), *Mechanism and theory in organic chemistry*, Harper & Row, New York, 3^{rd} edition
12. Taft, R. W. J. (1960), *J. Phys. Chem.* **64**, 1805–1815
13. Edmondson, D. E. and Ghisla, S. (1999), in Ghisla, S., Kroneck, P., Macheroux, P., and Sund, H., eds., *Flavins and Flavoproteins*, Rudolf Weber, Agency for Scientific Publications, Berlin, chapter 1, pp. 71–76
14. Barlow, J. N., Girvin, M. E., and Blanchard, J. S. (1999), *J. Am. Chem. Soc.* **121**, 6968–6969
15. Mullins, L. S. and Raushel, F. M. (1995), *Method. Enzymol.* **249**, 398–425